DOI: 10.14529/jsfi230102

Simulation of Isolated Propeller Noise Using Acoustic-Vortex Method

Mikhail A. Pogosyan[1]***, Sergey F. Timushev***[1]***, Petr A. Moshkov***[1]***, Alexey A. Yakovlev***[1]

The widespread development of unmanned aerial vehicles and light propeller-driven aircraft poses the task of reducing the community noise of such vehicles. To solve this problem, tools are needed to calculate the noise of such devices. The paper presents the results of the numerical simulation of the noise of an AV-2 propeller mounted on an AN-2 light propeller-driven aircraft. The authors use the acoustic-vortex method to solve the problem of aeroacoustic modeling of propeller noise in the presence of an incoming flow. The paper shows a good agreement of computed data with the in-flight experiment results and the calculation by the semi-empirical method. For the flight mode with an airspeed of 180 km/h, the deviation of the numerical simulation results from the experimental data does not exceed 2 dB.

Keywords: propeller noise, aeroacoustics, numerical simulation.

Introduction

The problem of numerical simulation of propeller noise is currently relevant due to the following factors:

- the vast development of the subject of uncrewed aerial vehicles (UAVs) [1–3];
- development of advanced configurations of aircraft with a distributed power plant [4, 5];
- development of open-rotor power plants and their integration into aircraft configuration.

For all the types of aircraft described above, the problem of controlling low noise levels to ensure certification and competitiveness is relevant. Several types of modern and promising aircraft configurations with propellers are shown in Fig. 1. Aeroacoustic effects may appear in the presented configurations, such as the noise of the blade-turbulent wake interaction [6, 7], the noise of the vortex blade interaction, the scattering of the power plant noise on the airframe elements [8, 9] and others. These effects must be considered when modeling aircraft noise and when implementing noise reduction technologies [10–12].

The work aims to verify the acoustic-vortex method in modeling the noise of an isolated propeller in the presence of an incoming flow (in-flight conditions). Preliminary verification was previously performed based on the results of static tests of the propeller-driven power plant, and the results are presented in [13].

The paper assumes that in the studied layout of AV-2 propeller on AN-2 aircraft, the propeller in flight conditions can be taken isolated.

The article is organized as follows. Section 1 presents object of study and test procedure for verification. Section 2 describes the numerical modeling method, presents the main equations, the calculated area and grid. Section 3 presents the results of numerical simulation of the aerodynamic and acoustic characteristics of the propeller. Section 4 presents a comparison of the results of numerical modeling with experimental data, as well as the results of calculation using a semi-empirical model.

[1]Moscow Aviation Institute (National Research University), Moscow, Russia

1. Object of Study and Test Procedure for Verification

The object of the study is an AV-2 propeller mounted on AN-2 light propeller-driven aircraft (LPDA). The main parameters of the aircraft and its power plant are presented in Tab. 1. The general view of the aircraft and its propeller is shown in Fig. 2.

Figure 1. Modern and advanced configurations of aircraft with propellers

Table 1. The main parameters of AN-2 light propeller-driven aircraft

Engine	ASH-62IR
Available power, kW	735.43
Displacement, l	29.86
Compression ratio	6.4
Power-to-volume ratio, kW/l	24.62
Specific power, kW/kg	1.31
Gear ratio	0.6875
Propeller	AV-2
Number of blades	4
Propeller diameter, m	3.6

The results of aeroacoustic modeling were compared with experimental data on the AV-2 propeller noise to verify the acoustic-vortex method. Flight tests of the aircraft were conducted with level cruising flight conditions at an altitude of 100 m. Table 2 presents the flight modes considered in the framework of this work to verify the numerical solution.

The tests were conducted at the local aerodrome of the Moscow Aviation Institute (National Research University) with an underlying surface in the form of mown grass. During tests, the measuring microphone was located so that the sensitive membrane was parallel to the round

(a)

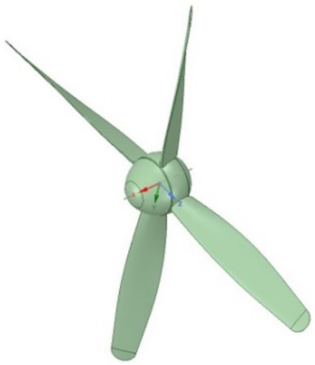

(b)

Figure 2. A general view of AN-2 aircraft (a) and its propeller AV-2 (b)

Table 2. Flight modes of AN-2 light propeller-driven aircraft for verifying the numerical solution

No.	Airspeed (V), km/h	Propeller speed (n), rpm
1	160	1100
2	180	1238

metal plate on the earth's surface and was placed 7 mm from it. The microphone was installed at a distance equal to three-fourths between the center and the edge of the plate along the radius and perpendicular to the flight path of LPDA. This microphone installation method is used in the certification tests of light propeller-driven aircraft. The ambient noise levels during the tests were lower than the noise levels of the power plant in the entire studied frequency range by at least 10–15 dB. The results of flight acoustic tests of AN-2 aircraft are presented in detail in [14].

2. Method of Numerical Simulation

2.1. Main Equations

Aeroacoustics modeling is based on decomposing compressible medium motion equations into the vortex (vortex motion of an incompressible medium) and acoustic modes [15, 16]. The velocity is the sum of the vortex flow velocity and the velocity of acoustic motion, which gives an acoustic-vortex equation for the fluctuations of the enthalpy ($\boldsymbol{i}$) in the isentropic flow of the compressible medium:

$$\frac{1}{a^2}\frac{\partial^2 i}{\partial t^2} - \Delta i = \nabla\left(\nabla(1/2 U^2) - U \times (\nabla \times U)\right), \tag{1}$$

where a – mean sound speed, U – the velocity field of the vortex mode (pseudo-sound).

The equations of moments are used to model the vortex mode:

$$\frac{\partial \rho U}{\partial t} + \nabla \cdot (\rho U \otimes U) = -\nabla P + \nabla \cdot \left((\mu + \mu_t)\left(2\widehat{S} - \frac{2}{3}(\nabla \cdot U)\widehat{I}\right)\right) \tag{2}$$

and continuity

$$\frac{\partial \rho}{\partial t} + \nabla(\rho \cdot U) = 0, \tag{3}$$

where ρ – air density, P – pressure in the vortex flow, μ – molecular coefficient of dynamic viscosity, μ_t – turbulent coefficient of dynamic viscosity, $\widehat{S}$ – strain rate tensor, $\widehat{I}$ – unit tensor.

The solution methodology discussed is based on the finite volume method. The finite volume method involves the integration of the equations of fluid motion and the transfer of scalar quantities in partial derivatives with respect to the volumes of computational cells – polyhedra. This ensures the conservatism of the mass, momentum, energy and other desired quantities in the computational domain. For the finite-difference solution of the equations of the vortex mode, the method of splitting by physical processes is used, which provides the second order of approximation accuracy in spatial variables and the first order in time. To solve the wave equation, an explicit method is used in time with the second order of approximation accuracy in space and time.

The acoustic-vortex method is implemented as a beta version of the single-processor software code FlowVision 2.5x. Currently, the development of a multiprocessor version of the acoustic-vortex module based on FlowVision 3.12 is being completed.

The k-e turbulence model determines the turbulent viscosity with setting of solid wall boundary condition in the form of "wall functions" (numerical implementation of the logarithmic law for the velocity profile in the boundary layer).

2.2. Calculated Area and Grid

The calculation is carried out on a grid of the third level of adaptation with the number of calculation cells of 230000. The calculation time on the Intel(R) Core (TM) i5-7400 CPU 3.00 GHz processor for solving the vortex mode equations from zero initial conditions is 40 hours.

The calculated area is a cylinder with a diameter of 20 m and a height of 20 m (Fig. 3). The propeller locates in the center of the computation domain. The calculation is carried out in a fixed coordinate system with a simulation of the propeller rotation.

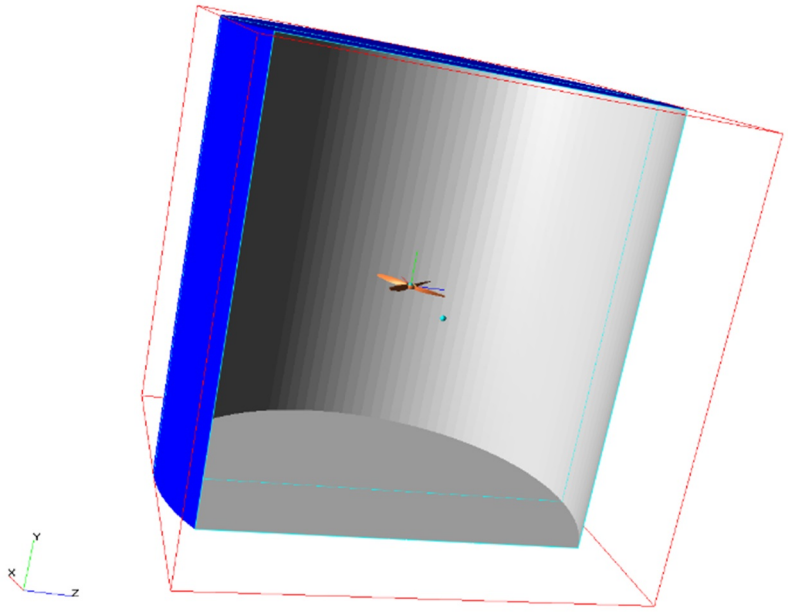

Figure 3. Computation region

In the computation study, an adapted grid of the third level is applied – near the propeller, the cells of the initial rectangular grid are divided into eight smaller cells – this procedure repeats three times. The computation grid in the vicinity of the propeller is shown in Fig. 4.

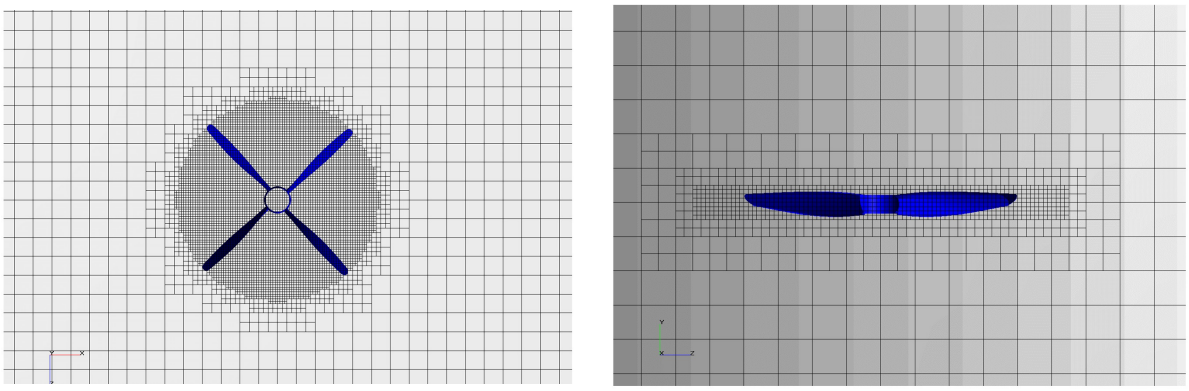

(a) in the plan view

(b) in the meridional plane

Figure 4. Computation grid

3. Results of Numerical Simulation

Numerical calculations were performed for two flight modes presented in Tab. 2. This section presents computational data on the airspeed of 180 km/h at a propeller speed of 1238 rpm.

3.1. Aerodynamic Results

The aerodynamic results are presented in Fig. 5 in the form of an instantaneous static pressure field (Pa) in the propeller rotation plane and the meridional plane.

One can see (Fig. 5a) that local pressure drop zones are formed when the propeller blades flow around. The propeller at work (Fig. 5b) throws off the flow and creates thrust, thus the aerodynamic pattern of the problem under consideration is realistic.

The results of the calculated evaluation of the thrust and power of the propeller for the flow conditions of the power plant considered in the work are presented in Tab. 3.

Table 3. Thrust and power of the propeller according to the results of numerical simulation

No.	Airspeed (V), km/h	Propeller speed (n), rpm	Thrust, N	Power, kW
1	160	1100	506.8	133.8
2	180	1238	315.8	139.3

3.2. Acoustic Results

The acoustic results in the sound pressure field (Pa) of the first BPF tone of propeller noise in the plane of rotation of the propeller and the meridional plane are shown in Fig. 6. The distribution of the amplitude (Pa) of the first BPF tone of propeller noise in the plane of rotation and the meridional plane is shown in Fig. 7.

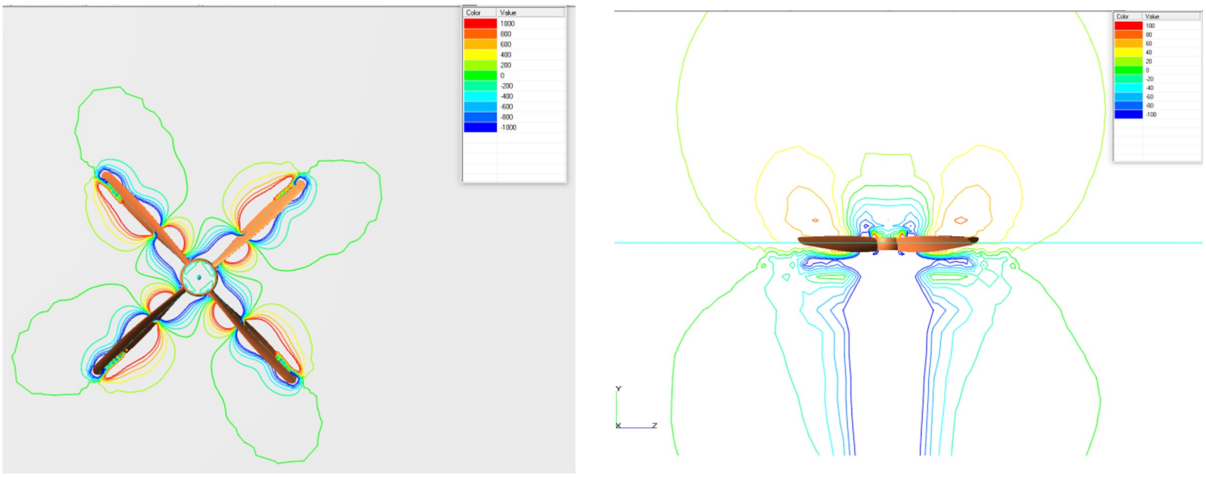

(a) in the plan view (b) in the meridional plane

Figure 5. Instantaneous static pressure field

The presented results indicate the dipole nature of the noise emission of the propeller [17, 18]. The maximum noise levels are observed in the direction of the azimuth angle of 90, which is consistent with the directional pattern of the first BPF tone of the studied propeller obtained under static conditions when the maximum was observed in the direction of 105 [13]. There are four characteristic directions of radiation maximums located symmetrically in the plane of rotation.

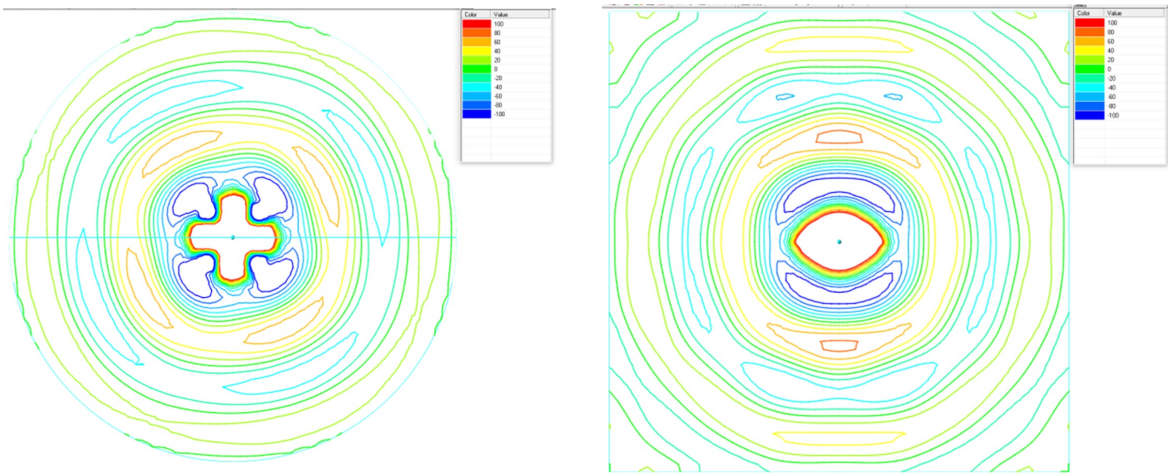

(a) in the plan view (b) in the meridional plane

Figure 6. Sound pressure field (Pa) of the 1st BPF tone of the propeller noise (flight direction along the Y-axis)

The distribution of sound pressure of the 1st BPF tone at the boundary of the calculation domain is shown in Fig. 8. The sound pressure is distributed unevenly and symmetrically on the lateral surface, revealing four maximums. One can see that at the inlet and outlet of the cylindrical region, the sound pressure is distributed evenly and decreases to the periphery.

4. Comparison of Calculated and Experimental Data

The comparison of calculated and experimental data is based on comparing the sound power levels of the first three tones of the propeller noise. The evaluation results are shown in Fig. 9

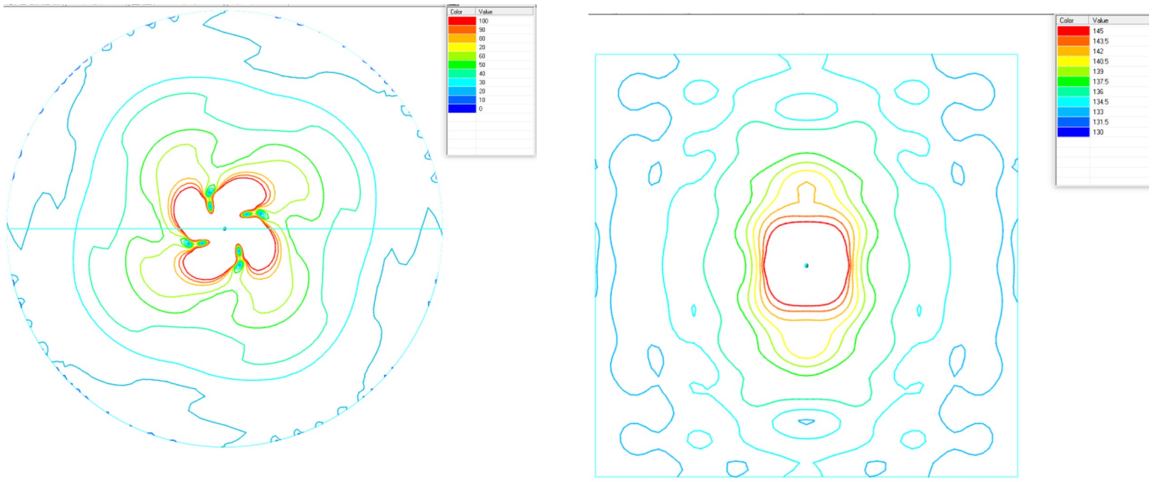

(a) in the plan view

(b) in the meridional plane

Figure 7. Amplitude (Pa) of the 1st BPF tone of the propeller noise (flight direction along the Y-axis)

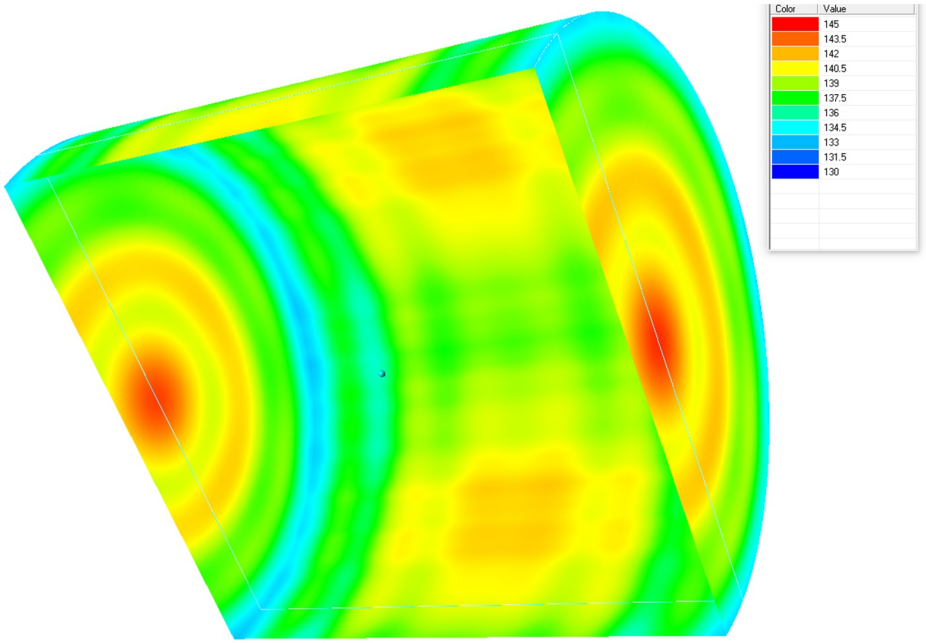

Figure 8. Sound pressure distribution (dB) of the first tone at the boundary of the computational region

for two flight modes. Additionally, the graph shows the results of the calculation performed by the semi-empirical method [19, 20].

For a flight mode with an airspeed of 160 km/h, a good agreement was obtained between the results of numerical simulation and experimental data for the first two tones of propeller noise. For the flight mode with a speed of 180 km/h, the deviation from the experimental data does not exceed 2 dB.

Note that the semiempirical method provides an acceptable calculation accuracy for solving engineering problems. For the two presented calculated cases, the deviation of the measured and calculated sound power levels of the above three tones does not exceed 2 dB.

According to the authors of the work, in this case, a deviation within 2 dB is a good result of modeling the sound field of a propeller, since the measurement error of the sound pressure level of the measuring system used is 0.7 dB. A deviation of more than 3 dB when assessing the sound power level leads to an overestimation or underestimation of the sound power by 2 times.

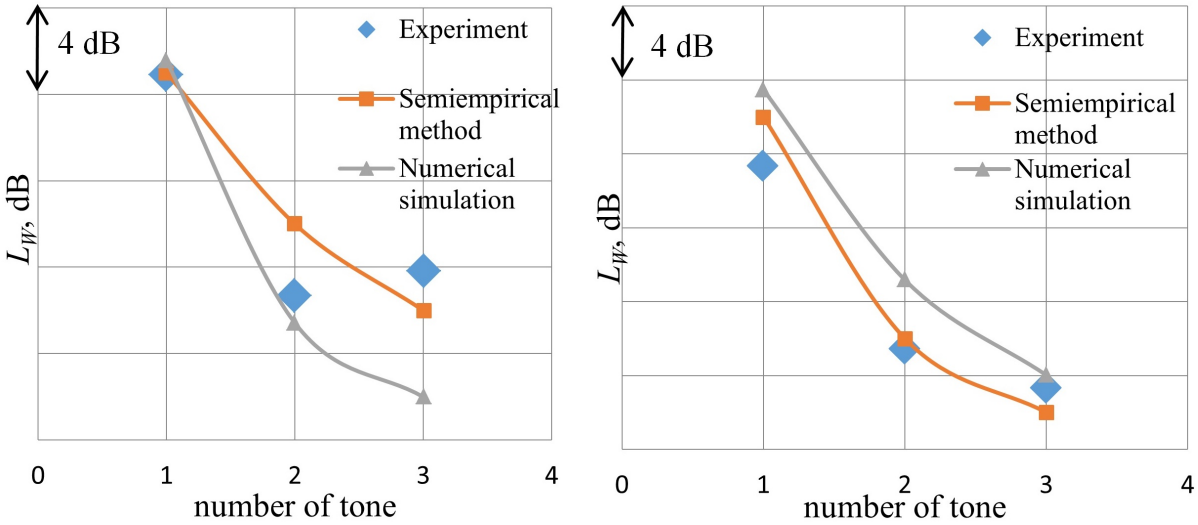

(a) $V = 160$ km/h, $n = 1100$ rpm (b) $V = 180$ km/h, $n = 1238$ rpm

Figure 9. Comparison of sound power levels of the first three propeller noise tones obtained in the experiment with numerical and semi-empirical modeling

Conclusions

A numerical simulation of the noise of the AV-2 propeller installed on AN-2 LPDA is performed. The calculations were performed for the cruising flight modes of the aircraft with airspeeds of 160 and 180 km/h corresponding to the propeller speeds of 1100 and 1238 rpm, respectively. The description of the acoustic-vortex method, the calculation area, and the computation grid are presented. The aerodynamic results are presented in a distribution of the instantaneous pressure field. The acoustic results are presented in the form of a sound pressure field and the amplitude of the first BPF tone of the propeller noise. The data indicates the dominance of dipole noise at the frequency of the first tone, that is, noise from a steady aerodynamic load. For the studied propeller, the thickness noise is insignificant in the flight modes considered, consistent with well-known propeller noise theories and experimental data.

The numerical simulation results are compared with the results of the in-flight experiment and the results of calculating the propeller noise by the semi-empirical method. The data obtained in the experiment agree with the results of numerical and semi-empirical modeling. Verification results indicate the possibility of using the acoustic-vortex method in solving the problem of computing the noise of propellers in tractor configurations. As a parameter for comparative evaluation, the sound power level for the first three tones at frequencies multiple of the blade passing frequency was selected. This parameter does not depend on the distance from the source and characterizes the propeller sound energy emission.

The presented work continues to investigate the possibility of using the acoustic-vortex method to simulate the propeller noise in actual aircraft configurations, considering the installation effects (blade-wake interaction noise, blade-vortex interaction noise, scattering noise of airframe elements, etc.).

Acknowledgements

The authors thank Kozhevnikov Yevgeniy, head of the Moscow Aviation Institute (National Research University) local aerodrome, for organizing acoustics tests.

References

1. Pettingill, N.A., Zawodny, N., Lopes, L.V.: Acoustic and Performance Characteristics of an Ideally Twisted Rotor in Hover. AIAA Scitech 2021 Forum, AIAA Paper No. 2021-1928 (2021). https://doi.org/10.2514/6.2021-1928

2. Yang, Y., Liu, Y., Li, Y., *et al.*: Aerodynamic and Aeroacoustic Performance of an Isolated Multicopter Rotor During Forward Flight. AIAA Journal 58(2) (2020). https://doi.org/10.2514/1.J058459

3. Zhou, T. Jiang, H., Sun, Y., *et al.*: Acoustic Characteristics of a Quad-Copter Under Realistic Flight Conditions. 25th AIAA/CEAS Aeroacoustics Conference, AIAA Paper No. 2019-2587 (2019). https://doi.org/10.2514/6.2019-2587

4. Moshkov, P., Samokhin, V., Yakovlev, A.: About the community noise problem of the light propeller aircraft. Akustika 34, 68–73 (2019). https://doi.org/10.36336/akustika20193466

5. Moshkov, P., Samokhin, V., Yakovlev, A., Bolun, C.: The problems of selecting the power plant for light propeller-driven aircraft and unmanned aerial vehicle taking into account the requirements for community noise. Akustika 39, 164–169 (2021). https://doi.org/10.36336/akustika202139162

6. Titarev, V.A., Faranosov, G.A., Chernyshev, S.A., Batrakov, A.S.: Numerical modeling of the influence of the relative positions of a propeller and pylon on turboprop aircraft noise. Acoust. Phys. 64, 760–773 (2018). https://doi.org/10.1134/S1063771018060118

7. Drofelnik, J., Andrejasic, M., Mocan, B., *et al.*: Measurement and modelling of aero-acoustic installation effects in tractor and pusher propeller architectures. 2021 AIAA AVIATION Forum, AIAA Paper No. 2021-2301 (2021). https://doi.org/10.2514/6.2021-2301

8. Vieira, A., Snellen, M., Malgoezar, A.M.N., Merino-Martinez, R., Simons, D.G.: Analysis of shielding of propeller noise using beamforming and predictions. JASA 146(2), 1085–1098 (2019). https://doi.org/10.1121/1.5121398

9. Vieira, A., Malgoezar, A., Snellen, M., Simons, D.G.: Experimental study of shielding of propeller noise by a wing and comparison with model predictions. Euronoise-2018, 237–244 (2018).

10. Rathgeber, R., Sipes, D.: The Influence of Design Parameters on Light Propeller Aircraft Noise. SAE Technical Paper No. 770444 (1977). https://doi.org/10.4271/770444

11. Dahan, C, Avezard, L., Guillien, G., *et al.*: Propeller Light Aircraft Noise at Discrete Frequencies. Journal of Aircraft 18(6), 480–486 (1981). https://doi.org/10.2514/3.57515

12. Berton, J.J., Nark, D.M.: Low-Noise Operating Mode for Propeller-Driven Electric Airplanes. Journal of Aircraft 56(4), 1708–1714 (2019). https://doi.org/10.2514/1.C035242

13. Timushev, S., Yakovlev, A., Moshkov, P.: Numerical simulation of the light aircraft propeller noise under static condition. Akustika 41, 100–106 (2021). https://doi.org/10.36336/akustika202141100

14. Moshkov, P.: Study of the influence of in-flight conditions on the light propeller-driven aircraft noise. Aerospace systems 5, 131–140 (2022). https://doi.org/10.1007/s42401-021-00127-5

15. Timushev, S., Klimenko, D., Aksenov, A., *et al.*: On a new approach for numerical modeling of the quadcopter rotor sound generation and propagation. Proceedings of 2020 International Congress on Noise Control Engineering, INTER-NOISE (2020).

16. Timushev, S., Yakovlev, A., Klimenko, D.: CFD-CAA Method for Prediction of Pseudosound and Emitted Noise in Quadcopter Propeller. International Journal of Modeling and Optimization 12(1), 21–25 (2022). https://doi.org/10.7763/IJMO.2022.V12.794

17. Herniczek, M.T.K., Feszty, D., Meslioui, S., Park, J.: Applicability of Early Acoustic Theory for Modern Propeller Design. 23rd AIAA/CEAS Aeroacoustics Conference, AIAA Paper No. 2017-3865 (2017). https://doi.org/10.2514/6.2017-3865

18. Herniczek, M.T.K., Feszty, D., Meslioui, S., *et al.*: Evaluation of Acoustic Frequency Methods for the Prediction of Propeller Noise. AIAA Journal 57(6) (2019). https://doi.org/10.2514/1.J056658

19. Samokhin, V.F.: Semiempirical method for estimating the noise of a propeller. Journal of Engineering Physics and Thermophysics 85(5), 1157–1166 (2012). https://doi.org/10.1007/s10891-012-0758-y

20. Moshkov, P.A, Samokhin, V.F.: Integral model of noise of an engine-propeller power plant. Journal of Engineering Physics and Thermophysics 91(2), 332–338 (2018). https://doi.org/10.1007/s10891-018-1753-8